BSM ν physics: complementarity across energies − a white paper for Snowmass 2021

Tao Han,[a] **Jiajun Liao,**[b] **Hongkai Liu,**[c] **Danny Marfatia,**[d,e] **Richard Ruiz**[f]

[a]*PITT PACC, Department of Physics and Astronomy,*
University of Pittsburgh, Pittsburgh, PA 15260, USA

[b]*School of Physics, Sun Yat-Sen University, Guangzhou, 510275, China*

[c]*Department of Physics, Technion – Israel Institute of Technology, Haifa 3200003, Israel*

[d]*Department of Physics and Astronomy, University of Hawaii at Manoa, Honolulu, HI 96822, USA*

[e]*Kavli Institute for Theoretical Physics, University of California, Santa Barbara, CA 93106, USA*

[f]*Institute of Nuclear Physics, Polish Academy of Sciences (IFJ PAN),*
ul. Radzikowskiego, Kraków 31-342, Poland

E-mail: than@pitt.edu, liaojiajun@mail.sysu.edu.cn, hol42@pitt.edu, dmarf8@hawaii.edu, rruiz@ifj.edu.pl

ABSTRACT: We reiterate that there is significant complementarity between low-energy experiments and high-energy colliders in exploring new physics associated with neutrino properties and their mass generation mechanisms. Signals of the new physics in the two energy regimes may be correlated with each other from the same underlying dynamics. We demonstrate the complementary nature by presenting the physics reaches for the Seesaw models of Type I, II and III, and for general neutrino interactions in an effective field theory framework, and in a Z' model.

Contents

1 Introduction

Flavor oscillations between massive neutrinos is a firmly established phenomenon that cannot be accounted for by the Standard Model (SM). Neutrino oscillations thus strongly motivate physics beyond the SM (BSM) that is associated with the neutrino sector. New physics associated with neutrinos can be probed at different energy scales and with limited theoretical prejudice. Certain signals of the new physics in the two energy regimes may be correlated with each other from the same underlying theory. It is ultimately important to seek complementary signals to establish a consistent picture of the underlying physics.

There are three tree-level mechanisms to generate neutrino masses of Majorana type that extend the SM's field content in a minimal manner [1]. All of these introduce new particle states, including ones with gauge charges, and thus lead to rich phenomenology, complementary in different experiments at all energy scales. Here, we summarize searches for testing these models at the Large Hadron Collider (LHC) and its upgrades. For wide-ranging reviews on tests of both tree-level and radiative neutrino mass models, see Refs. [2–4].

On the phenomenological ground, general neutrino interactions (GNI) is the most general parameterization of new physics in the neutrino sector and widely used at the low-energy probes. The effective four-fermion interactions are commonly written as

$$\mathscr{L}_{\mathrm{GNI}} = \frac{G_F}{\sqrt{2}} \sum_a (\bar{\nu}\Gamma_a \nu)[\bar{f}\Gamma_a(\epsilon_a + \tilde{\epsilon}_a \gamma^5)f], \tag{1.1}$$

where $\Gamma_a = \{\mathbb{1}, i\gamma^5, \gamma^\mu, \gamma^\mu\gamma^5, \sigma^{\mu\nu}\}$ are the five Lorentz structures, corresponding to scalar, pseudoscalar, vector, axialvector, and tensor interactions, respectively. f denotes quarks and charged leptons. ϵ and $\tilde{\epsilon}$ are the effective GNI parameters, and contain four flavor indices, which are kept implicit. The GNI is not valid above the weak scale or new physics scale. For illustration of the UV completion, we introduce a neutral gauge boson Z' to show the

effects at different energies. We then adopt an SM effective field theory formalism including a right-handed neutrino (νSMEFT/SMNEFT). We demonstrate that the low- and high-energy probes have their own merits based on Refs. [5–7].

2   Collider tests of tree-level seesaws

Collider experiments offer powerful probes of heavy states predicted by neutrino mass models. As benchmarks, direct tests of minimal tree-level scenarios typically focus on phenomenological implementations [8, 9] of the canonical Types I, II, and III Seesaw models. Phenomenological scenarios treat the masses and mixing of new particles states as independent parameters to minimize model dependence.

The Phenomenological Type I Seesaw extends the SM field content by $n_R \geq 2$ right-handed neutrinos ν_R. After electroweak (EW) symmetry breaking, the model parameterizes the mixing between EW currents and neutrino mass eigenstates by the decomposition

$$\nu_\ell = \sum_{m=1}^{3} U_{\ell m}^* \nu_m + \sum_{m'=4}^{3+n_R} V_{\ell m'}^* N_{m'}, \tag{2.1}$$

where ν_ℓ is a SM neutrino of flavor ℓ in the interaction basis, ν_m are the three light neutrino mass eigenstates, $U_{\ell m}$ are the light-active mixing matrix elements measured in oscillation experiments, $N_{m'}$ are heavy mass eigenstates, and $V_{\ell m'}$ are active-heavy (or active-sterile) mixing matrix elements. For discovery purposes, one typically considered only the $N_{m'=4}$ states and decouples the remaining $(n_R - 1)$ heavy mass eigenstates. The states N_k couple to EW bosons through mixing, and therefore can be produced in a variety of mechanisms. At the LHC, the leading channels are the Drell-Yan mechanism [10], $W\gamma$ fusion [11–14], gluon fusion [15–17], and same-sign $W^\pm W^\pm$ scattering [18, 19]. For recent comparisons of the channels at the LHC and beyond, see Refs. [14, 19, 20].

Figure 1 shows the 95% CL sensitivity to active-sterile mixing $|V_{\ell 4}|^2$ as a function heavy neutrino mass at the LHC in the trilepton and MET channel using the analysis of Refs. [20, 21] for the benchmark flavor categories: (a) $|V_{e4}|^2 = |V_{\mu 4}|^2$ with $|V_{\tau 4}|^2 = 0$, (b) $|V_{e4}|^2 = |V_{\tau 4}|^2$ with $|V_{\mu 4}|^2 = 0$, (c) $|V_{\mu 4}|^2 = |V_{\tau 4}|^2$ with $|V_{e4}|^2 = 0$. Depending on the precise flavor category, active-sterile mixing as small as $|V_{\ell N}|^2 \sim 10^{-4} - 10^{-2}$ can be reached for masses in the approximate range of $m_N \approx 200 - 1200$ GeV with 3 ab^{-1} of data [20, 21]. For some signal categories, the trilepton becomes directly competitive with low-energy tests of charged lepton flavor violation [22]. Fig. 1(d) shows the same but using the same-sign $W^\pm W^\pm \to \mu^\pm \mu^\pm$ scattering channel with the analysis of Ref. [19]. The analysis shows that mixing as small as $|V_{\ell N}|^2 \sim 10^{-1}$ can be reached for as large as $m_N \sim \mathcal{O}(10)$ TeV. It is important to stress that, if discovered, measuring heavy neutrinos' chiral couplings will be paramount to fully exploring their properties and potential couplings to other undiscovered particles [23–25].
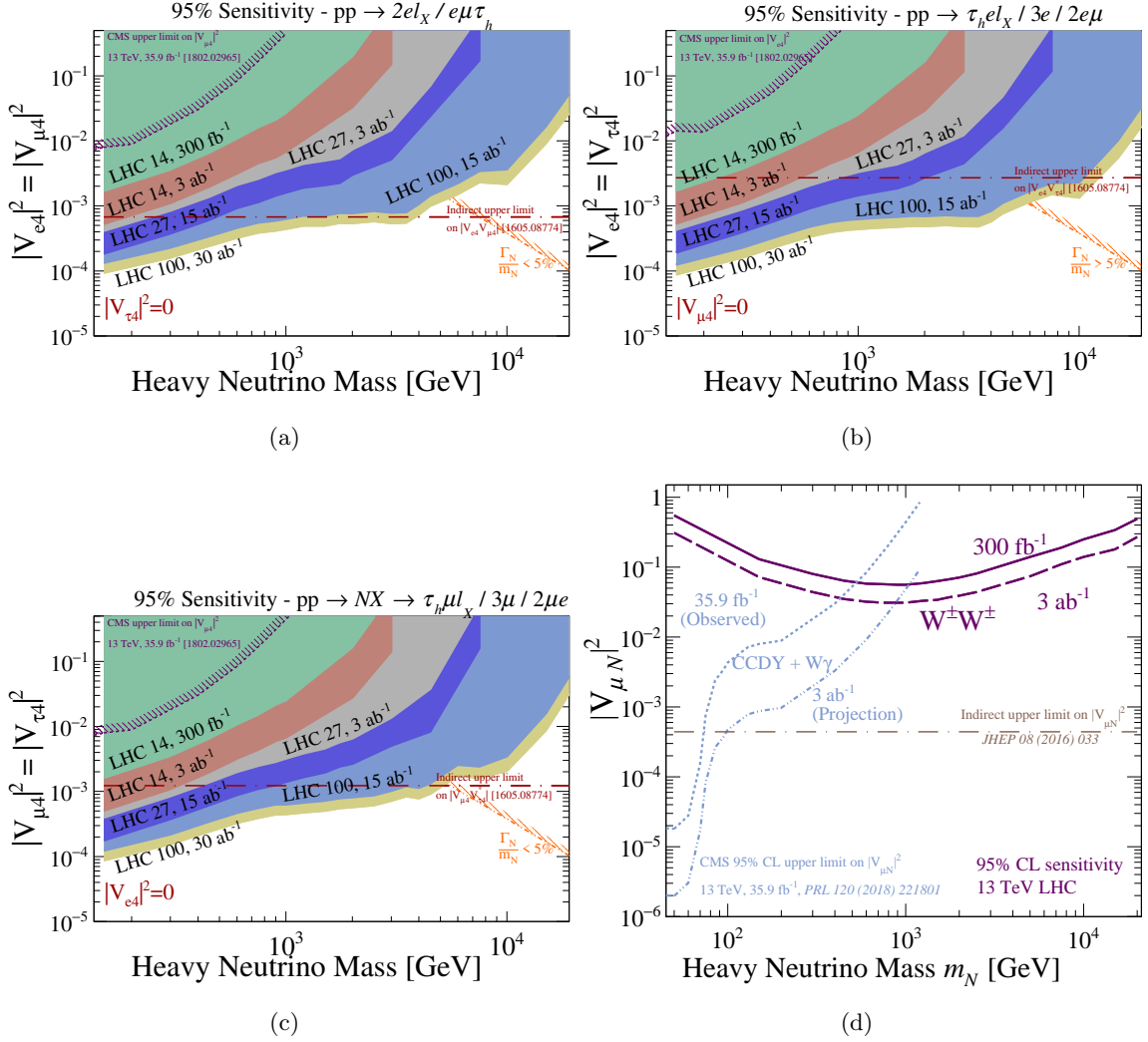
Figure 1. 95% CL sensitivity to active-sterile mixing $|V_{\ell 4}|^2$ as a function heavy neutrino mass at the LHC in the trilepton and MET channel using the analysis of Refs. [20, 21] for the benchmark flavor categories: (a) $|V_{e4}|^2 = |V_{\mu 4}|^2$ with $|V_{\tau 4}|^2 = 0$, (b) $|V_{e4}|^2 = |V_{\tau 4}|^2$ with $|V_{\mu 4}|^2 = 0$, (c) $|V_{\mu 4}|^2 = |V_{\tau 4}|^2$ with $|V_{e4}|^2 = 0$. (d) Same but using the same-sign $W^{\pm}W^{\pm} \to \mu^{\pm}\mu^{\pm}$ scattering channel with the analysis of Ref. [19].

The Type II Seesaw extends the SM field content by a scalar multiplet that is a triplet under $\mathrm{SU}(2)_L$ and carries hypercharge $Y = 1$. In the gauge basis, this can be written as

$$\sqrt{2}\hat{\Delta} = \begin{pmatrix} \hat{\Delta}^+ & \sqrt{2}\hat{\Delta}^{++} \\ \sqrt{2}\hat{\Delta}^0 & -\hat{\Delta}^+ \end{pmatrix}, \tag{2.2}$$

which couples at tree-level to the SM Higgs field, including through a dimension $d = 4$ operator that explicitly violates lepton number. After EW symmetry breaking, $\hat{\Delta}$ acquires a
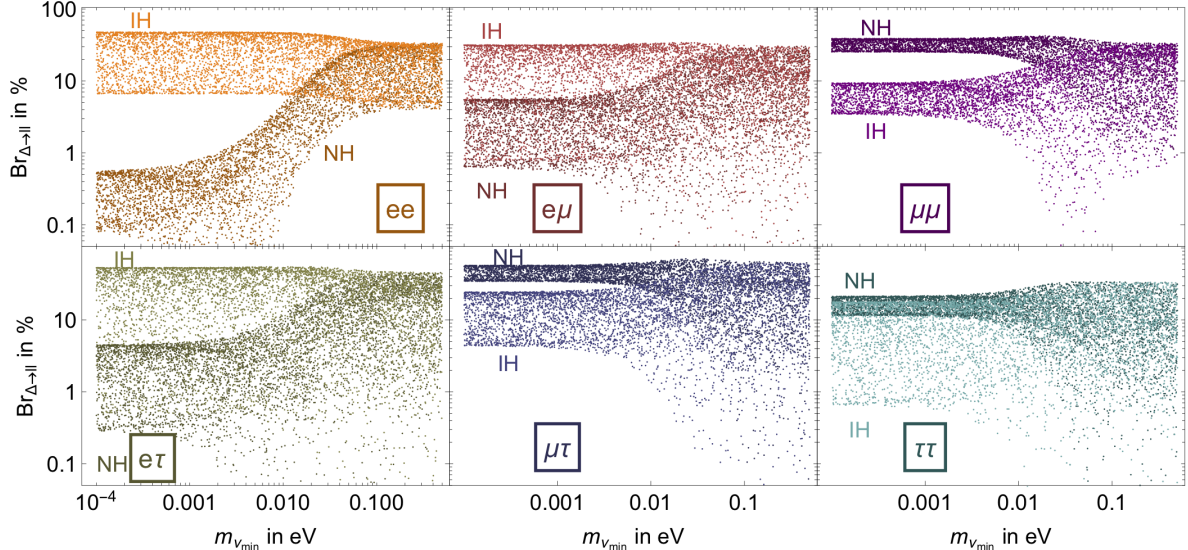
Figure 2. The branching rate (BR) of $\Delta^{\pm\pm} \to \ell_i^\pm \ell_j^\pm$ decays in the Type II Seesaw as a function of the lightest neutrino mass for the normal hierarchy (NH) and inverted hierarchy (IH) ordering of neutrino masses, and in the limit of a vanishing triplet vev. Adapted from Ref. [26].

vacuum expectation value (vev) and spontaneously generates left-handed Majorana masses for neutrinos through a Yukawa coupling. Importantly, this is an instances of generating neutrino masses without right-handed neutrinos.

After mixing with the SM Higgs, the Type II Seesaw predicts the existence of four new scalar, mass eigenstates: a doubly electrically charged Higgs $\Delta^{\pm\pm}$, a singly electrically charged Higgs $\Delta^\pm$, an electrically neutral CP-even Higgs Δ^0, and an electrically neutral CP-odd Higgs ξ^0. These new states carry EW gauge couplings and can be produced through variety of tree- and loop-induced processes [26, 27]. For a recent comparison of these channels at the LHC and future proton colliders, see Ref. [26].

Due to the absence of sterile neutrinos, the flavor structure and mass pattern of neutrinos are entirely set by the Yukawa couplings between $\hat{\Delta}$ and the leptonic doublets of the SM. This means that the decay rates of $\Delta^{\pm\pm}$, $\Delta^\pm$, Δ^0, and ξ^0 to leptons, which are proportional to Yukawa couplings, are strongly constrained by the PMNS matrix, and hence neutrino oscillation data [28]. For the case of $\Delta^{\pm\pm}$, Fig. 2 shows [26] the branching rate (BR) of $\Delta^{\pm\pm} \to \ell_i^\pm \ell_j^\pm$ decays as a function of the lightest neutrino mass for the normal hierarchy (NH) and inverted hierarchy (IH) ordering of neutrino masses, in the limit of a vanishing triplet vev. The correlations predicted for the decay fractions of Type II scalars highlights the complementarity of oscillation experiments and high-energy collider experiments.

Using the analyses of Refs. [8, 26, 28], and as a function of triplet scalar masses, Fig. 3(a) shows the luminosity required to reach 5σ (3σ) discovery (sensitivity) of triplet scalars produced in pairs at the LHC and subsequently decay to multi-lepton final states. (Also shown is
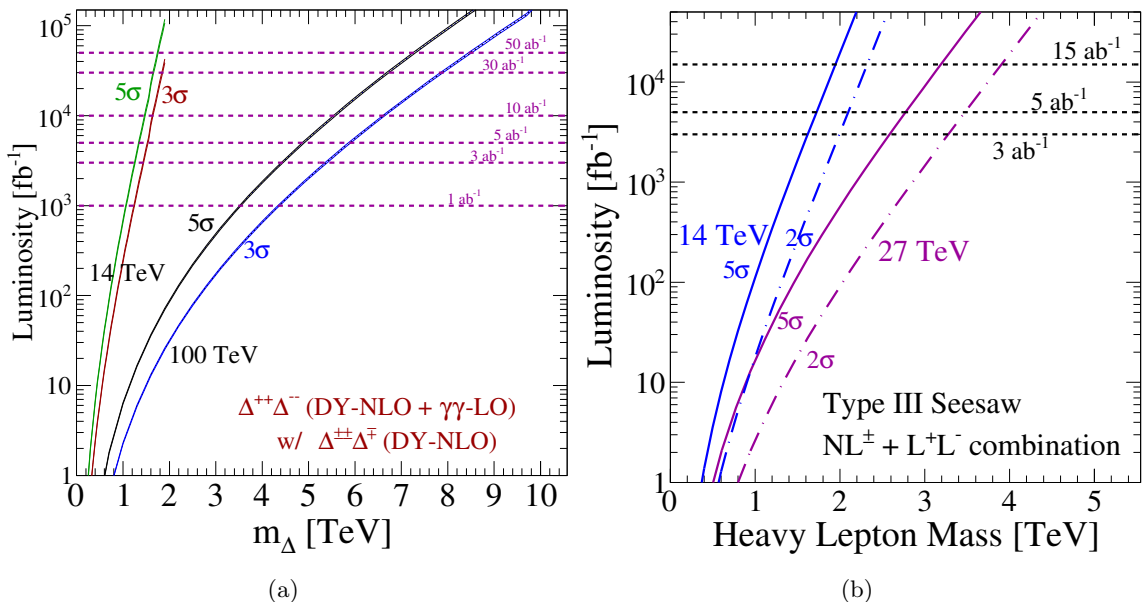
Figure 3. (a) The luminosity required to reach 5σ (3σ) discovery (sensitivity) of Type II Seesaw scalars produced in pairs produced in $\sqrt{s} = 14$ and 100 TeV pp collisions, and which subsequently decay to multi-lepton final states. Adapted from Ref. [26]. (b) The same but for Type III leptons produced in pairs in $\sqrt{s} = 14$ and 27 TeV pp collisions. Adapted from Ref. [29].

the analogous sensitivity at a hypothetical 100 TeV pp collider.) At the LHC, pairs of triplet scalars with masses in the TeV range can be discovered with the full HL-LHC data set.

The Phenomenological Type III Seesaw extends the SM field content by $n_R \geq 2$ leptonic multiplets Σ that are triplets under $SU(2)_L$. Like the Type I Seesaw, Dirac neutrino masses are generated through Yukawa couplings involving the SM Higgs field, SM lepton doublets, and Σ. The neutral component of Σ also carries a Majorana mass, thereby triggering a high- or low-scale Seesaw depending on model assumptions. After mass diagonalization, the mass eigenstates $N, L^\pm$ can couple to charged and neutral leptons through mixing. The decomposition of gauge states into mass states can be parameterized by [30]

$$\Sigma^\pm = Y\ L^\pm + \varepsilon_T\ \ell^\pm \quad \text{and} \quad \Sigma^0 = Y\ N + \varepsilon_T\ \nu_m, \tag{2.3}$$

where $|Y| \sim \mathcal{O}(1)$ and $|\varepsilon_T| \ll 1$ are mixing parameters. With these couplings, Type III leptons can mediate lepton flavor violation in various low-energy observables [31, 32].

Due to their gauge couplings, triplet leptons can be produced in pairs directly from gauge interactions and through a variety of production mechanisms at proton colliders [4, 16, 29, 30]. Single production in association with a SM lepton is possible through mixing. For recent comparisons of individual channels at the LHC and beyond, see Refs [4]. Typically, decays of N and $L^\pm$ occurs at tree-level to SM leptons and an EW boson via mixing. However, even in the degenerate limit, $L^\pm \to N\pi^\pm$ decays are possible at one loop [33, 34]. Such decays

are allowed even in the limit of vanishing mixing. Using the analyses of Refs. [8, 29, 30, 35], Fig. 3(b) shows the luminosity required to reach 5σ (3σ) discovery (sensitivity) of Type III Seesaw leptons produced in pairs produced in $\sqrt{s} = 14$ and 27 TeV pp collisions, and which subsequently decay to multi-lepton final states.

The Weinberg operator at the LHC. Neutrinoless $\beta\beta$ decay $(0\nu\beta\beta)$ experiments are powerful probes of lepton number violation and particularly the Weinberg operator

$$O^{\alpha\beta} = \left[\Phi \cdot \overline{L}_\alpha^c\right]\left[L_\beta \cdot \Phi\right]. \tag{2.4}$$

Here, Φ and L are the usual SM Higgs and lepton doublets, with flavor indicies α, β. Despite their incredible sensitivity, a limitation of $0\nu\beta\beta$ decay experiments is their flavor dependence. These experiments are only sensitive to phenomena in the $\ell_\alpha\ell_\beta = ee$ channel, and the production of same-sign lepton pairs involving muons or taus is kinematically forbidden.

As noted in Ref. [36], the high-p_T analogue of the $0\nu\beta\beta$ process is the same-sign $W^\pm W^\pm \to \ell_\alpha^\pm\ell_\beta^\pm$ scattering channel, and is potentially accessible at the LHC. A full signal-versus-background analysis shows that the $\sqrt{s} = 13$ TeV LHC with $\mathcal{L} = 300$ ab^{-1} (3 ab^{-1}) can exclude EFT cutoff scales below $\Lambda \lesssim 8.3$ (11) TeV for a Wilson coefficient of $C^{\alpha\beta} = 1$ in the flavor channel $\ell_\alpha\ell_\beta = \mu\mu$ [36]. Anticipated sensitivity to the $\ell_\alpha\ell_\beta = ee$ and $e\mu$ channels is anticipated to be comparable, with degraded sensitivity to the $\ell_\alpha\ell_\beta = \tau\tau, \tau e$ and $\tau\mu$ to the smaller τ lepton identification. It is possible to extend this an analysis to the decays of heavy and light mesons [36, 37], thereby bringing further complementarity between high- and low-energy probes of BSM in the neutrino sector.

3 Z' model

In this section, we discuss a scenario where the new physics scale is not high compared to the EW scale and therefore cannot be integrated out in low-energy tests. We focus on a Z' model associated with a new, anomaly-free $U(1)'$ symmetry. For concreteness, we consider masses in the range $M_{Z'} = 5$ MeV to few TeV and its coupling $g' < 1$. The Lagrangian can be written as

$$\mathscr{L} = \mathscr{L}_{\mathrm{SM}} - \frac{1}{4}Z'^{\mu\nu}Z'_{\mu\nu} + \frac{1}{2}M_{Z'}^2 Z'^\mu Z'_\mu + Z'_\mu J_X^\mu, \tag{3.1}$$

where J_X^μ is the fermion current that couples to the Z' boson. For the sake of illustration, we take the following three cases for our benchmark studies [38]:

$$(A)\ Z_{B-3L_\mu}, \quad (B)\ Z_{B-\frac{3}{2}(L_\mu+L_\tau)}, \quad (C)\ Z_{B-3L_\tau}.$$

The parameters in these models can be constrained by both low-energy probes, like neutrino oscillation and coherent elastic neutrino-nucleus scattering, and high-energy probes like the collider experiments. The results are shown in Fig. 4. The red shaded areas and dashed lines correspond to the 2σ exclusion regions by using the energy spectrum from the COHERENT CsI detector [39] and the expected 2σ limit from COHERENT with a 750 kg LAr detector and a 4-year exposure using both energy and time information [40], respectively.
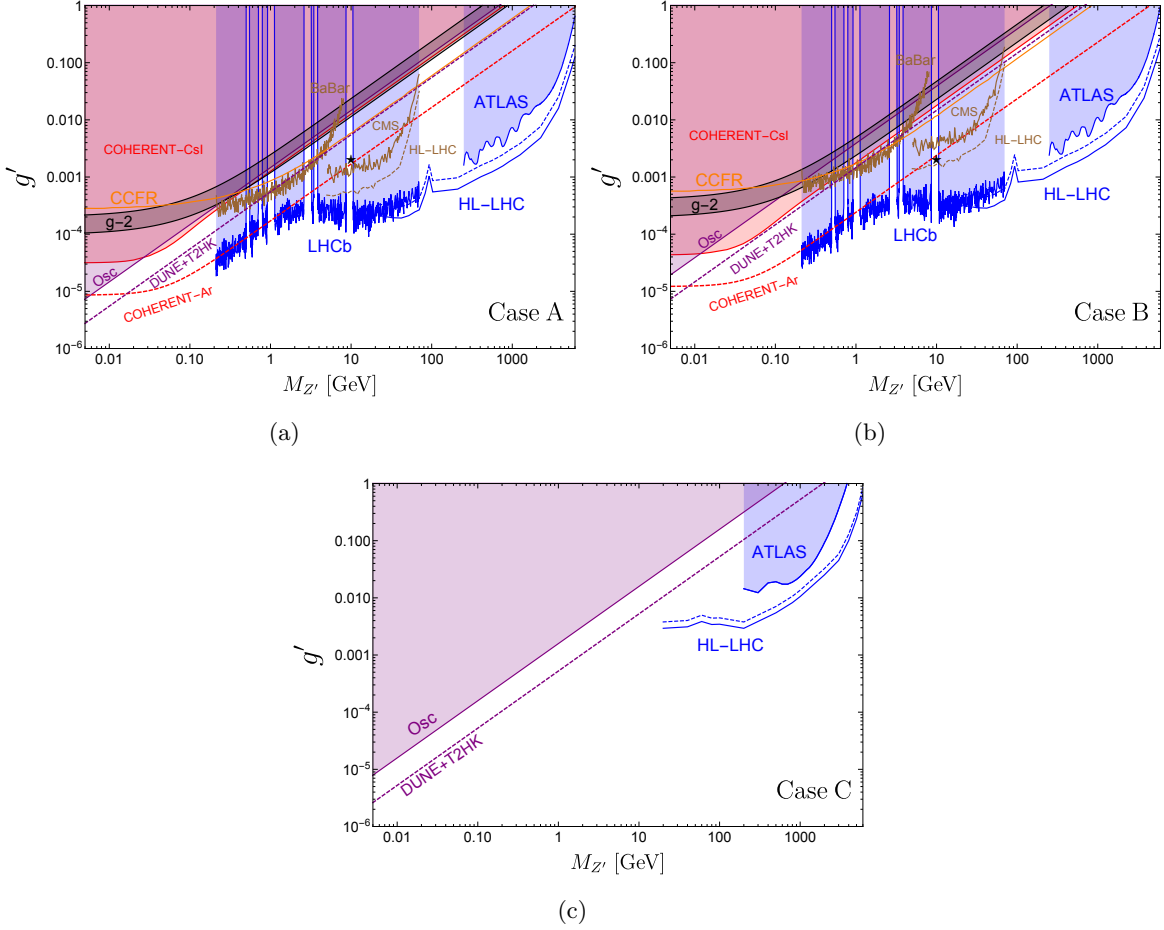
Figure 4. Bounds on g' as a function of $M_{Z'}$ for Cases A (upper left panel), B (upper right panel) and C (lower panel). For details of individual experiment, see Sec. 3.

The purple shaded areas and dashed lines correspond to the 2σ bounds from a global fit to neutrino oscillation data [41] and the expected 2σ exclusion limit from DUNE and T2HK combined, respectively. Regions above the brown curves are excluded by using $pp/e^+e^- \to \mu^+\mu^- Z'$ searches at CMS [42] and BaBar [43] at 2σ and 90% CL, respectively. The brown dashed curves are the 2σ expected sensitivities from the $\mu^+\mu^- Z'$ channel at HL-LHC, with an integrated luminosity of 3 ab^{-1}. The blue solid (dashed) curves correspond to the expected 2σ (5σ) limit using di-muon searches for Cases A and B, and di-tau searches for Case C. The blue shaded regions in the upper panels are excluded at 90% CL by the LHCb dark photon searches [44] and at 2σ by the ATLAS di-muon searches [45] with 139 fb^{-1}. The blue area in the lower panel is excluded at 2σ by the ATLAS di-tau searches [46] with 36.1 fb^{-1}. The orange curves correspond to the 2σ limit from CCFR [47, 48], and the black bands show the 2σ allowed regions that explain the discrepancy in the anomalous magnetic moment of the muon ($\Delta a_\mu = (29 \pm 9) \times 10^{-10}$ [49]).

The low- and high-energy probes are complementary to search for a wide range of Z' masses. For Z' masses above 10 GeV, the ATLAS and CMS experiments at HL-LHC have the best sensitivity regardless of the flavor structure of the model. For masses between $0.01\,\mathrm{GeV}-10\,\mathrm{GeV}$, current LHCb data and future COHERENT data have the best sensitivity unless the Z' couplings to the first and second generation leptons are suppressed, in which case neutrino oscillation experiments have the best sensitivity. For Z' masses between about $5\,\mathrm{MeV}-20\,\mathrm{MeV}$, DUNE and T2HK have the best sensitivity.

4 νSMEFT / SMNEFT

When the new physics scale is much higher than the weak scale, an EFT framework that is consistent with the SM gauge symmetries can be used above the weak scale. To parameterize scenarios where the mass of a heavy neutrino state is comparable to the EW scale but the scale of GNI is much larger than both, it is possible to extend the SM by right-handed neutrinos and build an effective field theory based on the given field content. The framework, known as νSMEFT or SMNEFT, reduces to the familiar SMEFT when heavy neutrinos are integrated out of the theory [50–52]. Thus, νSMEFT is a broader framework than SMEFT and can generate GNI at low energies. We focus on four operators:

1. $O_{NLQu}^{\alpha\beta\gamma\delta} = (\overline{N}_\alpha L_\beta^j)(\overline{Q}_\gamma^j u_\delta)$,

2. $O_{NLdQ}^{\alpha\beta\gamma\delta} = (\overline{N}_\alpha L_\beta^j)\epsilon_{jk}(\overline{d}_\gamma Q_\delta^k)$,

3. $O_{NLdQ}'^{\alpha\beta\gamma\delta} = (\overline{N}_\alpha \sigma_{\mu\nu} L_\beta^j)\epsilon_{jk}(\overline{d}_\gamma \sigma^{\mu\nu} Q_\delta^k)$,

4. $O_{HNe} = \left(i\tilde{\varphi}^\dagger D_\mu \varphi\right)\overline{N}\sigma^\mu e_R$,

where the fields are written in two-component spinors. L and Q are the left-handed lepton and quark doublet, respectively, φ is the left-handed Higgs doublet, and N is the right-handed neutrino state. Here, $\sigma^{\mu\nu} = \frac{i}{2}[\sigma^\mu \overline{\sigma}^\nu - \sigma^\nu \overline{\sigma}^\mu]$, with $\sigma^\mu = (\mathbb{1}, \vec{\sigma})$ and $\overline{\sigma}^\mu = (\mathbb{1}, -\vec{\sigma})$. RG running is needed to combine the results from various energy scales and it has been calculated in Refs. [6, 53–55]. Generally there are degeneracies between νSMEFT Wilson coefficients at low-energy observables due to the running effects. High-energy measurements can break the degeneracies. Low-energy probes and high-energy colliders are complementary to probe various type of interactions as shown in Fig. 5.

If EW-scale sterile neutrinos contribute to the anomalous magnetic moments of charged leptons, then it is possible to parameterize their impact with the νSMEFT framework [7]. Notably, only one operator at dimension $d = 6$ can account for the difference between recent measurements and predictions for the muon's anomalous magnetic moment, Δa_μ. In particular, with the exception of operator O_{HNe} above, all other operators at $d = 6$ either generate too small or too large Δa_μ [7]. Moreover, the measured value of Δa_μ is sufficiently large that the allowed band of (C_{HNe}/Λ) and m_N, with realistic active-sterile mixing is accessible at
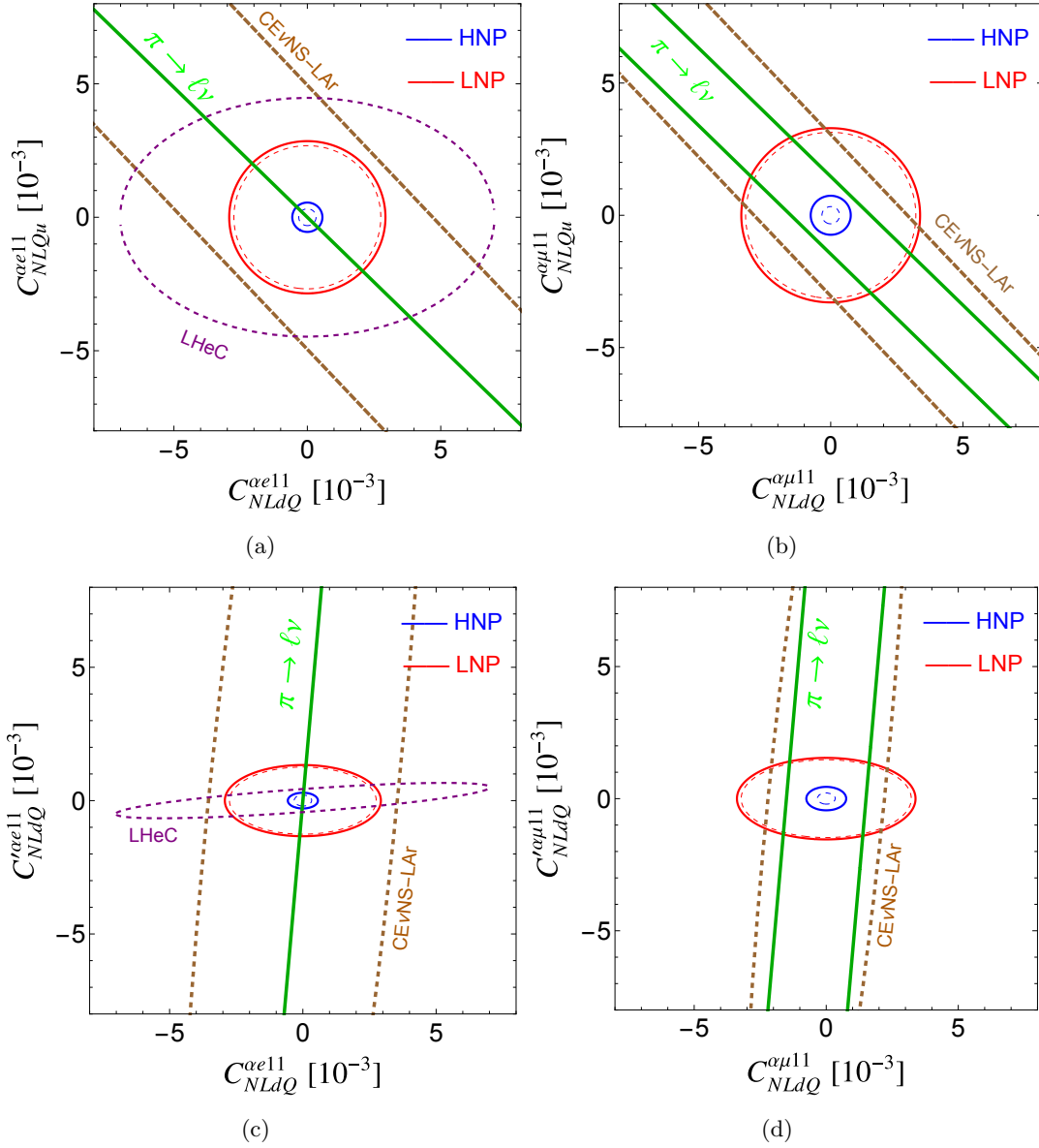
Figure 5. The 90% C.L. allowed regions in the C_{NLdQ}-C_{NLQu} planes (upper panels) and C_{NLdQ}-C'_{NLdQ} planes (lower panels) at 1 TeV with $\ell = e$ flavor (left) and $\ell = \mu$ flavor (right). The green lines (overlapping in the left panels) correspond to the bounds from pion decay with the third parameter set to zero to break the degeneracy. The red (blue) solid contours show current LHC searches with $L = 139\,\mathrm{fb}^{-1}$ for the low-scale new physics LNP (high-scale new physics HNP) case. The brown dashed lines correspond to the projected bounds from the future LAr COHERENT experiment, with C_{NLQu} is set to zero in the lower panels to obtain meaningful bounds. The red and blue dashed contours are the projected bounds from HL-LHC with $3\,\mathrm{ab}^{-1}$ of data for the LNP and HNP case, respectively. The dashed purple contours in the left panels correspond to the projected bounds from LHeC with $3\,\mathrm{ab}^{-1}$.
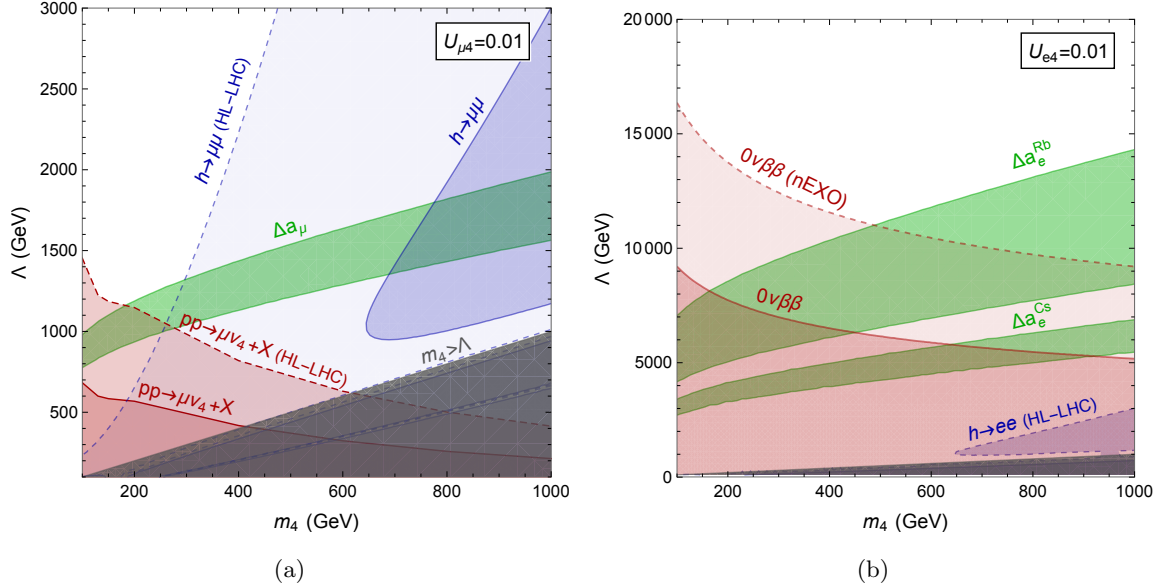
Figure 6. (a) For a Wilson coefficient of unity and active-sterile mixing $|U_{\mu 4}|^2 = 10^{-4}$, the region in (Λ, m_4) space that can account for the measured value of Δa_μ (green band); current exclusions due to direct searches for sterile neutrinos (dark red) and $H \to \mu^+\mu^-$ decays (dark blue) at $\sqrt{s} = 13$ TeV; the anticipated sensitivity at the HL-LHC in the same channels (light red and light blue); and exclusions due to requiring $m_4 < \Lambda$. (b) Same as (a) but for $\ell = e$ with present constraints (dark red) as well as anticipated sensitivity from $0\nu\beta\beta$ experiments (light red) and searches for $H \to e^+e^-$ at the HL-LHC. Figure adapted from Ref. [7].

the LHC. (Here, C_{HNe} is the Wilson coefficient for O_{HNe}, Λ is the EFT cutoff scale, m_4 is the mass of the heavy mass eigenstate N.)

For a Wilson coefficient of unity and active-sterile mixing $|U_{\mu 4}|^2 = 10^{-4}$, Fig. 6(a) shows the region in (Λ, m_4) space that can account for the measured value of Δa_μ (green band); current exclusions due to direct searches for sterile neutrinos with $\mathcal{L} \approx 36$ fb^{-1} (dark red) [] and $H \to \mu^+\mu^-$ decays with $\mathcal{L} \approx 137$ fb^{-1} (dark blue) [56, 57] at $\sqrt{s} = 13$ TeV; the anticipated sensitivity at the HL-LHC in the same channels (light red and light blue) [58]; and exclusions due to requiring $m_4 < \Lambda$. By the end of the HL-LHC program, nearly the entire allowed parameter space can be explored at the HL-LHC [7].

A disagreement between experimental determinations of the electron's anomalous magnetic moment using Cesium [59] and Rubidium [60] also exists. While inaccessible at the HL-LHC, the nEXO neutrinoless $\beta\beta$ ($0\nu\beta\beta$) decay experiment [61] will be able to explore much of the allowed (Λ, m_4) space. This is shown in Fig. 6(b), where the allowed space for Δa_e is shown as are present constraints (dark red) as well as anticipated sensitivity from $0\nu\beta\beta$ experiments (light red) and searches for $H \to e^+e^-$ at the HL-LHC based on current exclusions [62]. Figure adapted from Ref. [7].

Finally, other studies in the νSMEFT framework report sensitivity at the LHC to indi-

vidual operators at the LHC [24, 50, 51, 63–66] as well as proposed lepton colliders [67–70].

5   Executive summary

Through a few phenomenological examples, we reiterate that there is significant complementarity between low-energy experiments (such as DUNE) and high-energy collider experiments (such as the LHC) in exploring new physics associated with neutrino properties and their mass-generation mechanisms. Signals of new physics in the two energy regimes may be correlated with each other in the same underlying theory. We demonstrate the complementary nature by presenting the physics reaches for the Seesaw models of Type I, II and III, and for general neutrino interactions in an effective field theory framework, and in a Z' model. It is crucially important to seek complementary signals to establish a consistent picture of the underlying physics associated with the mechanisms responsible for generating neutrino masses.

References

[1] E. Ma, *Pathways to naturally small neutrino masses*, *Phys. Rev. Lett.* **81** (1998) 1171–1174, [`hep-ph/9805219`].

[2] F. F. Deppisch, P. S. Bhupal Dev and A. Pilaftsis, *Neutrinos and Collider Physics*, *New J. Phys.* **17** (2015) 075019, [`1502.06541`].

[3] Y. Cai, J. Herrero-García, M. A. Schmidt, A. Vicente and R. R. Volkas, *From the trees to the forest: a review of radiative neutrino mass models*, *Front. in Phys.* **5** (2017) 63, [`1706.08524`].

[4] Y. Cai, T. Han, T. Li and R. Ruiz, *Lepton Number Violation: Seesaw Models and Their Collider Tests*, *Front. in Phys.* **6** (2018) 40, [`1711.02180`].

[5] T. Han, J. Liao, H. Liu and D. Marfatia, *Nonstandard neutrino interactions at COHERENT, DUNE, T2HK and LHC*, *JHEP* **11** (2019) 028, [`1910.03272`].

[6] T. Han, J. Liao, H. Liu and D. Marfatia, *Scalar and tensor neutrino interactions*, *JHEP* **07** (2020) 207, [2004.13869].

[7] V. Cirigliano, W. Dekens, J. de Vries, K. Fuyuto, E. Mereghetti and R. Ruiz, *Leptonic anomalous magnetic moments in ν SMEFT*, *JHEP* **08** (2021) 103, [2105.11462].

[8] F. del Aguila and J. A. Aguilar-Saavedra, *Distinguishing seesaw models at LHC with multi-lepton signals*, *Nucl. Phys. B* **813** (2009) 22–90, [0808.2468].

[9] A. Atre, T. Han, S. Pascoli and B. Zhang, *The Search for Heavy Majorana Neutrinos*, *JHEP* **05** (2009) 030, [0901.3589].

[10] W.-Y. Keung and G. Senjanovic, *Majorana Neutrinos and the Production of the Right-handed Charged Gauge Boson*, *Phys. Rev. Lett.* **50** (1983) 1427.

[11] A. Datta, M. Guchait and A. Pilaftsis, *Probing lepton number violation via majorana neutrinos at hadron supercolliders*, *Phys. Rev. D* **50** (1994) 3195–3203, [hep-ph/9311257].

[12] P. S. B. Dev, A. Pilaftsis and U.-k. Yang, *New Production Mechanism for Heavy Neutrinos at the LHC*, *Phys. Rev. Lett.* **112** (2014) 081801, [1308.2209].

[13] D. Alva, T. Han and R. Ruiz, *Heavy Majorana neutrinos from Wγ fusion at hadron colliders*, *JHEP* **02** (2015) 072, [1411.7305].

[14] C. Degrande, O. Mattelaer, R. Ruiz and J. Turner, *Fully-Automated Precision Predictions for Heavy Neutrino Production Mechanisms at Hadron Colliders*, *Phys. Rev. D* **94** (2016) 053002, [1602.06957].

[15] D. A. Dicus and P. Roy, *Supercollider signatures and correlations of heavy neutrinos*, *Phys. Rev. D* **44** (1991) 1593–1596.

[16] A. G. Hessler, A. Ibarra, E. Molinaro and S. Vogl, *Impact of the Higgs boson on the production of exotic particles at the LHC*, *Phys. Rev. D* **91** (2015) 115004, [1408.0983].

[17] R. Ruiz, M. Spannowsky and P. Waite, *Heavy neutrinos from gluon fusion*, *Phys. Rev. D* **96** (2017) 055042, [1706.02298].

[18] D. A. Dicus, D. D. Karatas and P. Roy, *Lepton nonconservation at supercollider energies*, *Phys. Rev. D* **44** (1991) 2033–2037.

[19] B. Fuks, J. Neundorf, K. Peters, R. Ruiz and M. Saimpert, *Majorana neutrinos in same-sign $W^{\pm}W^{\pm}$ scattering at the LHC: Breaking the TeV barrier*, *Phys. Rev. D* **103** (2021) 055005, [2011.02547].

[20] S. Pascoli, R. Ruiz and C. Weiland, *Heavy neutrinos with dynamic jet vetoes: multilepton searches at $\sqrt{s} = 14$, 27, and 100 TeV*, *JHEP* **06** (2019) 049, [1812.08750].

[21] S. Pascoli, R. Ruiz and C. Weiland, *Safe Jet Vetoes*, *Phys. Lett. B* **786** (2018) 106–113, [1805.09335].

[22] E. Fernandez-Martinez, J. Hernandez-Garcia and J. Lopez-Pavon, *Global constraints on heavy neutrino mixing*, *JHEP* **08** (2016) 033, [1605.08774].

[23] T. Han, I. Lewis, R. Ruiz and Z.-g. Si, *Lepton Number Violation and W' Chiral Couplings at the LHC*, *Phys. Rev. D* **87** (2013) 035011, [1211.6447].

[24] R. Ruiz, *Lepton Number Violation at Colliders from Kinematically Inaccessible Gauge Bosons*, *Eur. Phys. J. C* **77** (2017) 375, [`1703.04669`].

[25] R. Ruiz, *Quantitative study on helicity inversion in Majorana neutrino decays at the LHC*, *Phys. Rev. D* **103** (2021) 015022, [`2008.01092`].

[26] B. Fuks, M. Nemevšek and R. Ruiz, *Doubly Charged Higgs Boson Production at Hadron Colliders*, *Phys. Rev. D* **101** (2020) 075022, [`1912.08975`].

[27] M. Nemevšek, F. Nesti and J. C. Vasquez, *Majorana Higgses at colliders*, *JHEP* **04** (2017) 114, [`1612.06840`].

[28] P. Fileviez Perez, T. Han, G.-y. Huang, T. Li and K. Wang, *Neutrino Masses and the CERN LHC: Testing Type II Seesaw*, *Phys. Rev. D* **78** (2008) 015018, [`0805.3536`].

[29] R. Ruiz, *QCD Corrections to Pair Production of Type III Seesaw Leptons at Hadron Colliders*, *JHEP* **12** (2015) 165, [`1509.05416`].

[30] A. Arhrib, B. Bajc, D. K. Ghosh, T. Han, G.-Y. Huang, I. Puljak et al., *Collider Signatures for Heavy Lepton Triplet in Type I+III Seesaw*, *Phys. Rev. D* **82** (2010) 053004, [`0904.2390`].

[31] A. Abada, C. Biggio, F. Bonnet, M. B. Gavela and T. Hambye, *Low energy effects of neutrino masses*, *JHEP* **12** (2007) 061, [`0707.4058`].

[32] J. F. Kamenik and M. Nemevsek, *Lepton flavor violation in type I + III seesaw*, *JHEP* **11** (2009) 023, [`0908.3451`]. [Erratum: JHEP 03, 033 (2014)].

[33] M. Ibe, T. Moroi and T. T. Yanagida, *Possible Signals of Wino LSP at the Large Hadron Collider*, *Phys. Lett. B* **644** (2007) 355–360, [`hep-ph/0610277`].

[34] A. Strumia and F. Vissani, *Neutrino masses and mixings and...*, `hep-ph/0606054`.

[35] T. Li and X.-G. He, *Neutrino Masses and Heavy Triplet Leptons at the LHC: Testability of Type III Seesaw*, *Phys. Rev. D* **80** (2009) 093003, [`0907.4193`].

[36] B. Fuks, J. Neundorf, K. Peters, R. Ruiz and M. Saimpert, *Probing the Weinberg operator at colliders*, *Phys. Rev. D* **103** (2021) 115014, [`2012.09882`].

[37] A. Atre, V. Barger and T. Han, *Upper bounds on lepton-number violating processes*, *Phys. Rev. D* **71** (2005) 113014, [`hep-ph/0502163`].

[38] J. Heeck, M. Lindner, W. Rodejohann and S. Vogl, *Non-Standard Neutrino Interactions and Neutral Gauge Bosons*, *SciPost Phys.* **6** (2019) 038, [`1812.04067`].

[39] COHERENT collaboration, D. Akimov et al., *Observation of Coherent Elastic Neutrino-Nucleus Scattering*, *Science* **357** (2017) 1123–1126, [`1708.01294`].

[40] COHERENT collaboration, D. Akimov et al., *COHERENT 2018 at the Spallation Neutron Source*, `1803.09183`.

[41] I. Esteban, M. C. Gonzalez-Garcia, M. Maltoni, I. Martinez-Soler and J. Salvado, *Updated constraints on non-standard interactions from global analysis of oscillation data*, *JHEP* **08** (2018) 180, [`1805.04530`]. [Addendum: JHEP 12, 152 (2020)].

[42] CMS collaboration, A. M. Sirunyan et al., *Search for an $L_\mu - L_\tau$ gauge boson using $Z \to 4\mu$ events in proton-proton collisions at $\sqrt{s} =$ 13 TeV*, *Phys. Lett. B* **792** (2019) 345–368, [`1808.03684`].

[43] BABAR collaboration, J. P. Lees et al., *Search for a muonic dark force at BABAR*, *Phys. Rev. D* **94** (2016) 011102, [1606.03501].

[44] LHCB collaboration, R. Aaij et al., *Search for $A' \to \mu^+\mu^-$ Decays*, *Phys. Rev. Lett.* **124** (2020) 041801, [1910.06926].

[45] ATLAS collaboration, G. Aad et al., *Search for high-mass dilepton resonances using 139 fb^{-1} of pp collision data collected at $\sqrt{s} = 13$ TeV with the ATLAS detector*, *Phys. Lett. B* **796** (2019) 68–87, [1903.06248].

[46] ATLAS collaboration, M. Aaboud et al., *Search for additional heavy neutral Higgs and gauge bosons in the ditau final state produced in 36 fb^{-1} of pp collisions at $\sqrt{s} = 13$ TeV with the ATLAS detector*, *JHEP* **01** (2018) 055, [1709.07242].

[47] CCFR collaboration, S. R. Mishra et al., *Neutrino tridents and W Z interference*, *Phys. Rev. Lett.* **66** (1991) 3117–3120.

[48] W. Altmannshofer, S. Gori, M. Pospelov and I. Yavin, *Neutrino Trident Production: A Powerful Probe of New Physics with Neutrino Beams*, *Phys. Rev. Lett.* **113** (2014) 091801, [1406.2332].

[49] F. Jegerlehner and A. Nyffeler, *The Muon g-2*, *Phys. Rept.* **477** (2009) 1–110, [0902.3360].

[50] F. del Aguila, S. Bar-Shalom, A. Soni and J. Wudka, *Heavy Majorana Neutrinos in the Effective Lagrangian Description: Application to Hadron Colliders*, *Phys. Lett. B* **670** (2009) 399–402, [0806.0876].

[51] S. Bhattacharya and J. Wudka, *Dimension-seven operators in the standard model with right handed neutrinos*, *Phys. Rev. D* **94** (2016) 055022, [1505.05264]. [Erratum: Phys.Rev.D 95, 039904 (2017)].

[52] Y. Liao and X.-D. Ma, *Operators up to Dimension Seven in Standard Model Effective Field Theory Extended with Sterile Neutrinos*, *Phys. Rev. D* **96** (2017) 015012, [1612.04527].

[53] A. Datta, J. Kumar, H. Liu and D. Marfatia, *Anomalous dimensions from gauge couplings in SMEFT with right-handed neutrinos*, *JHEP* **02** (2021) 015, [2010.12109].

[54] M. Chala and A. Titov, *One-loop running of dimension-six Higgs-neutrino operators and implications of a large neutrino dipole moment*, *JHEP* **09** (2020) 188, [2006.14596].

[55] A. Datta, J. Kumar, H. Liu and D. Marfatia, *Anomalous dimensions from Yukawa couplings in SMNEFT: four-fermion operators*, *JHEP* **05** (2021) 037, [2103.04441].

[56] CMS collaboration, A. M. Sirunyan et al., *Evidence for Higgs boson decay to a pair of muons*, *JHEP* **01** (2021) 148, [2009.04363].

[57] ATLAS collaboration, G. Aad et al., *A search for the dimuon decay of the Standard Model Higgs boson with the ATLAS detector*, *Phys. Lett. B* **812** (2021) 135980, [2007.07830].

[58] M. Cepeda et al., *Report from Working Group 2: Higgs Physics at the HL-LHC and HE-LHC*, *CERN Yellow Rep. Monogr.* **7** (2019) 221–584, [1902.00134].

[59] R. H. Parker, C. Yu, W. Zhong, B. Estey and H. Müller, *Measurement of the fine-structure constant as a test of the Standard Model*, *Science* **360** (2018) 191, [1812.04130].

[60] L. Morel, Z. Yao, P. Cladé and S. Guellati-Khélifa, *Determination of the fine-structure constant with an accuracy of 81 parts per trillion*, *Nature* **588** (2020) 61–65.

[61] EXO-200 collaboration, G. Anton et al., *Search for Neutrinoless Double-β Decay with the Complete EXO-200 Dataset*, *Phys. Rev. Lett.* **123** (2019) 161802, [1906.02723].

[62] ATLAS collaboration, G. Aad et al., *Search for the Higgs boson decays $H \to ee$ and $H \to e\mu$ in pp collisions at $\sqrt{s} = 13$ TeV with the ATLAS detector*, *Phys. Lett. B* **801** (2020) 135148, [1909.10235].

[63] A. Aparici, K. Kim, A. Santamaria and J. Wudka, *Right-handed neutrino magnetic moments*, *Phys. Rev. D* **80** (2009) 013010, [0904.3244].

[64] L. Duarte, J. Peressutti and O. A. Sampayo, *Majorana neutrino decay in an Effective Approach*, *Phys. Rev. D* **92** (2015) 093002, [1508.01588].

[65] G. Cottin, J. C. Helo, M. Hirsch, A. Titov and Z. S. Wang, *Heavy neutral leptons in effective field theory and the high-luminosity LHC*, *JHEP* **09** (2021) 039, [2105.13851].

[66] R. Beltrán, G. Cottin, J. C. Helo, M. Hirsch, A. Titov and Z. S. Wang, *Long-lived heavy neutral leptons at the LHC: four-fermion single-N_R operators*, *JHEP* **01** (2022) 044, [2110.15096].

[67] L. Duarte, I. Romero, J. Peressutti and O. A. Sampayo, *Effective Majorana neutrino decay*, *Eur. Phys. J. C* **76** (2016) 453, [1603.08052].

[68] L. Duarte, J. Peressutti and O. A. Sampayo, *Not-that-heavy Majorana neutrino signals at the LHC*, *J. Phys. G* **45** (2018) 025001, [1610.03894].

[69] L. Duarte, G. Zapata and O. A. Sampayo, *Final taus and initial state polarization signatures from effective interactions of Majorana neutrinos at future e^+e^- colliders*, *Eur. Phys. J. C* **79** (2019) 240, [1812.01154].

[70] G. Zapata, T. Urruzola, O. A. Sampayo and L. Duarte, *Lepton collider probes for Majorana neutrino effective interactions*, 2201.02480.